

## STUDY OF VEHICLE DYNAMIC MODELING FIDELITY ON HAPTIC COLLABORATION IN STEER-BY-WIRE SYSTEMS

**Anand P. Naik**

Mechanical and Aerospace  
Engineering  
State University of New York at  
Buffalo  
apnaik@eng.buffalo.edu  
<http://www.eng.buffalo.edu/~apnaik>

**Leng-Feng Lee**

Mechanical and Aerospace  
Engineering  
State University of New York at  
Buffalo  
llee3@eng.buffalo.edu  
<http://www.eng.buffalo.edu/~llee3>

**Venkat N. Krovi**

Mechanical and Aerospace  
Engineering  
State University of New York at  
Buffalo  
vkrovi@eng.buffalo.edu  
<http://www.eng.buffalo.edu/~vkrovi>

### ABSTRACT

The Steer-By-Wire (SBW) paradigm for vehicle control offers many advantages over traditional use of mechanical steering systems but comes at the cost of loss of proprioception (“road feel”). To this end, haptic interfaces for SBW systems have been proposed to restore the intimacy of interactive control back to the driver. However, the degree of realism for the interaction is dependent on the fidelity of the underlying computational vehicle dynamics model. Hence we focus on quantitative comparative testing of the role of vehicle dynamics modeling fidelity for haptic SBW tasks.

Additionally the SBW paradigm can simplify implementation of shared/collaborative control (steering) of the underlying mechanical system (vehicle). Possibilities range from sharing of control between multiple individual users or between user and automation technology. Performance evaluation of 3 modes of shared control vs. individual control of driving was carried out and preliminary analysis of results is presented in the paper.

### 1. INTRODUCTION

The focus of this work is on implementation and testing of a haptic-enabled Steer-by-Wire system (SBW) for vehicle driving applications. Steer-by-wire technology is characterized by the absence of mechanical linkages between the output steered vehicle tires and the input steering interfaces (usually a hand wheel or a joystick). Instead, the inputs and outputs are electronically connected through a system of sensors actuators, a communication network and an electronic controller [1]. There are numerous economic, safety and performance benefits accruing from the SBW paradigm [2, 3] that have driven the automotive industry’s efforts to replace conventional steering systems with intelligent mechatronic SBW solutions.

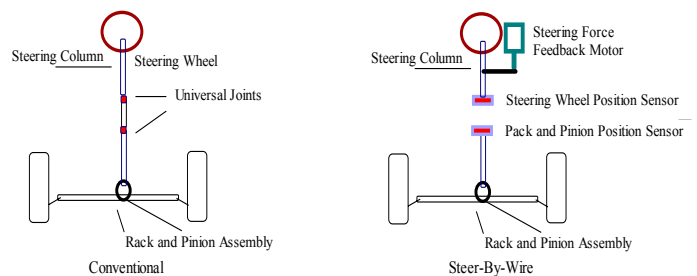


Figure 1: Conventional vs. Steer-By-Wire Steering System

For example, the absence of a steering column greatly simplifies car interior design and allows much better engine compartment space utilization. Furthermore, the entire steering mechanism can be designed and installed as a modular unit on either the left or right side. In the absence of a direct mechanical connection between the steering wheel and the road wheels, the noise, vibration, and harshness (NVH) from the road wheel interaction can no longer propagate to the driver’s hands and arms. Safety is significantly improved because of reduced likelihood of steering column intrusion into the driver’s survival space in case of front impacts. Finally, perhaps the greatest contributions to safety come about by the use of sensing and automation to modulate the driver vehicle interactions. There is considerable research interest in developing adaptive steering system to augment Adaptive Braking System (ABS) and Adaptive Cruise Control (ACC) for future vehicles.

However, there is a loss of proprioception (“road feel”) associated with steer-by-wire systems, which can be a valuable information channel facilitating vehicle control by human driver. Hence there is considerable incentive for reincorporation of force or haptic feedback to help restore the

“road feel”. The challenge is to develop mathematical models for hand-wheel torque feedback which would provide the requisite tunable realistic steering feel in the absence of mechanical linkages [4, 5]. In addition, such haptic feedback also provides exciting opportunities for modulating (amplifying, deamplifying, filtering and creating artificial feedback assists) force feedback presented to the driver. In particular, sharing of control between multiple users may now be easily incorporated within a haptic SBW paradigm.

The multitude of challenges to successful implementation of haptic assist in SBW system can be broadly categorized into three main areas: User, Human User Interface (HUI) and Virtual Environment as shown in Figure 2.

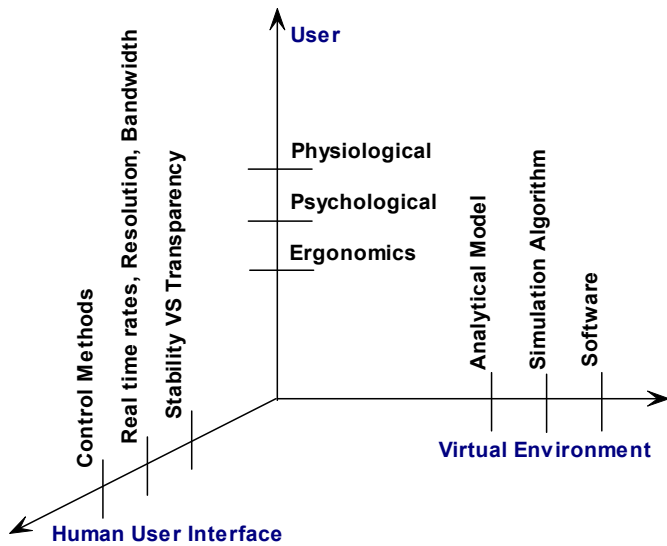


Figure 2: Challenges faced in three major areas

Along the “User Axis” the biomechanical, sensorimotor and cognitive abilities of humans play a vital role in governing the overall interaction performance. Our work will not focus much on this aspect but a broad overview of research challenges entailed here can be seen in [6]. On the “HUI Axis” the underlying mechanical properties of the hardware (viscosity, friction, mass) together with the selection of control methods (impedance, admittance) serve to modulate the interaction between the human user and the virtual environment. Transparency and stability are used as metrics of performance of HUI’s but these tend to place conflicting requirements. Thus one of the challenges is selection of suitable tradeoff between the stability and transparency via selection of device and control characteristics, real-time rates, instrumentation requirements [7-9].

The third axis pertains to the “Virtual Environment” that computes motion/force interaction in response to user inputs and disturbances. In our case, it corresponds to the mathematical model of vehicle dynamics and the computation of steering feel (torques/motions) in response to driver/road inputs.

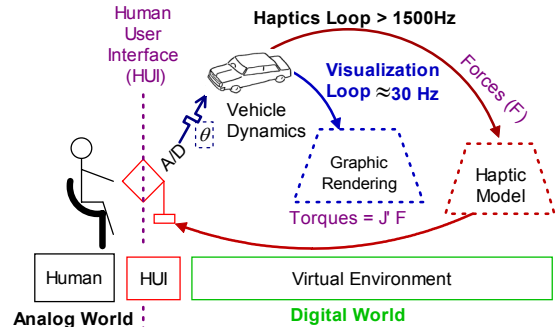


Figure 3: Refresh rate challenges

A careful selection of complexity of the underlying dynamic model as well as good matching of haptic model-device capabilities is critical and this serves to focus our research efforts. Specifically, we will first study the effects of use of varied fidelity of vehicle dynamics models on a user’s performance of driving. These models will range from a simple torsional-spring-mass damper model to a complex 14 degree of freedom full-car-ride model. Additionally the results/effects of collaboration between multiple users or between user and automation needs to be evaluated. Hence we also present preliminary results from user performance testing with both varied fidelity of vehicle control as well as varied modes of collaboration.

The rest of the paper is organized as follows: Section 2 discusses vehicle dynamics model development as well as validation. Section 3 presents details of the analytical modeling of multi-user collaboration modes. An overview of the implementation framework is given in Section 4. Section 5 discusses critical aspects of the experimental setup followed by analysis of the results. Section 6 concludes the paper.

## 2. VEHICLE DYNAMIC MODELS

### Model Development:

An articulated multi-body (AMB) vehicle model is created from groups of tires, links, joints springs, dampers and actuators that form the various subsystems of the vehicle. The driver provides the principal sets of control inputs to the system in the form of acceleration, break position, and steering angles (via a suitable driver interface). The road surface with various tunable parameters (such as surface roughness, stiffness, slope, curvature) is presumed to act as a disturbance input to the vehicle. Numerical simulation methods for AMB simulations now permit computation of vehicle’s dynamic performance, in response to these inputs, which can be fed back to the user.

It is noteworthy that the driver interface may have mechanical, hydraulic and electrical or electronic components. However the inner electronic and hydraulic control loops have much faster closed loop time constants than the mechanical components and can be replaced by corresponding zeroth order models i.e. as constant gains. Thus we will only focus on

developing dynamic steering system models based only on the articulated mechanical subsystems.

Candidate solutions for mimicking the steering feel [9-17] have ranged from direct instrumented-pickup and feedback of road-wheel interactions (using accelerometers/ force-sensors) to steering torque prediction schemes based on mathematical dynamics models (of tire-road, suspension, power-steering systems) in conjunction with selected real-time measurements. While the latter set of approaches offer the greatest promise from the view point of accuracy and fidelity, real-time implementations at high sampling rates in noisy environments pose challenges. It is well understood that real time operations at high sample rates are easier to achieve with lower fidelity models. However, there is little or no prior work examining the role of modeling fidelity or user control. Hence in this work we first focus on creating analytical models at four fidelity (Models A, B, C and D) for all human interface studies of driving along varied courses at constant speed.

**Model A:**

Model A in Figure 4(a) is comprised of three rotational bodies, namely, steering wheel, vehicle and tire connected via set of a torsional springs and dampers  $k_i, b_i \forall i=1,2$  whose values should be appropriately selected to provide the requisite steering feel. The governing system equation can be written as follows:

$$J \cdot \ddot{\delta} = k_1(\theta - \delta) + b_1(\dot{\theta} - \dot{\delta}) - k_2(\delta) - b_2(\dot{\delta}) \quad (1)$$

Note that in this case we have lumped vehicle and tire bodies as one single inertia body. The human is allowed to apply a prescribed motion profile at the steering wheel, which in this case translates to providing  $\theta$  and  $\dot{\theta}$ , the steering angle and steering velocity respectively and  $J$  represents the moment of inertia of the vehicle-tires subsystem. Thus the steering torque felt at the steering wheel can be represented by Equation(2):

$$\tau = k_1(\theta - \delta) + b_1(\dot{\theta} - \dot{\delta}) = T_{VA} \quad (2)$$

**Model B:**

Our second model is the well known bicycle model (Figure 4(b)) used in vehicle dynamics literature [15-18]. The governing system equations can be written as follows,

$$\ddot{y} = \frac{\sum F_y}{m} - \dot{\psi}u, \quad \ddot{\psi} = \frac{aF_{yF} - bF_{yR}}{I_Z} \quad (3)$$

where  $\ddot{y}, \ddot{\psi}$  represent the lateral acceleration and yaw rate change respectively. (Further details of the redevelopment of the analytical equations can be found in [19]). This model can now be used to explicitly compute the forces/ moments experienced at the road/ tire.

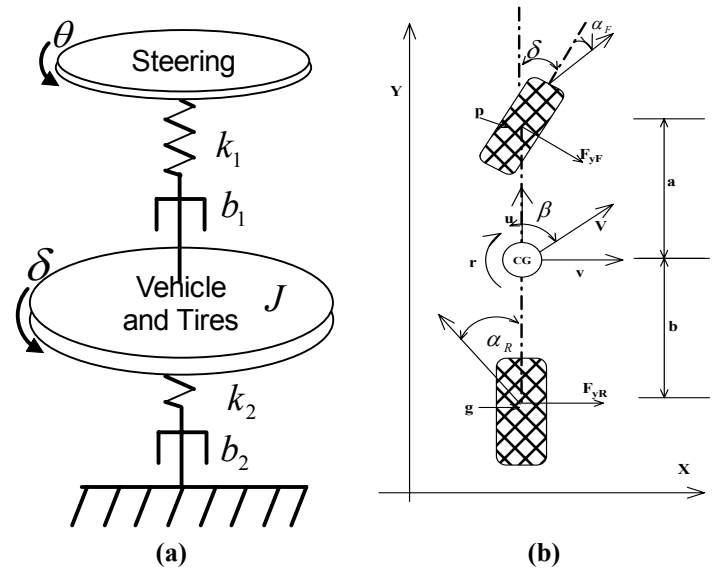


Figure 4: (a) Unicycle Model (Model A) and (b) The Bicycle Model (Model B).

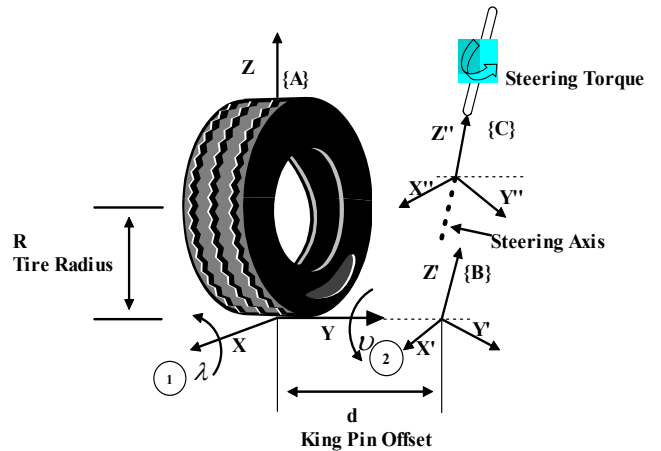


Figure 5: Steering Axis Location

The influence of these forces and moments at the tire can then be translated to the steering axis to determine the steering torque experienced about  $Z''$  (Figure 5) and provide an explicit model for steering feel as shown in [19]:

$$M_Z'' = -d \sin(\nu) \cos(\lambda) F_Z + \cos(\lambda) F_y \delta d \cos(\nu) + \cos(\nu) \cos(\lambda) M_Z + F_y \delta R \sin(\lambda) = T_{VB} \quad (4)$$

Equation (4) is the steering torque experienced by the driver when modeled using the bicycle model (Model B).

**Model C:**

It is readily apparent that developing complex articulated multi-body system equations can be very arduous and subject to human coding errors. For example, the development of

governing system equations even for small DOF models (such as Model A & B) requires careful formulation and meticulous coding. To alleviate, we employed DynaFlexPro, an add-on toolbox for Maple that can be used for developing the analytical equations of motion and subsequently simulating mechanical multi-body systems. Equations of motion of large degree of freedom (DOF) mechanical systems can be symbolically derived without the expense of time and hand coding. DynaFlexPro allows the users to also incorporate various latest pneumatic tire models into simulations of vehicle systems [20]. Figure 6 and 7 show the models which have 10 and 14 degree of freedom respectively. The base model in this car is the full 14 DOF model including the four independent vertical motions at each of the tires which we will refer to as Model D. Alternately the suspension effects from this 14 DOF can be eliminated to create a 10 DOF Model that we will refer to as Model C.

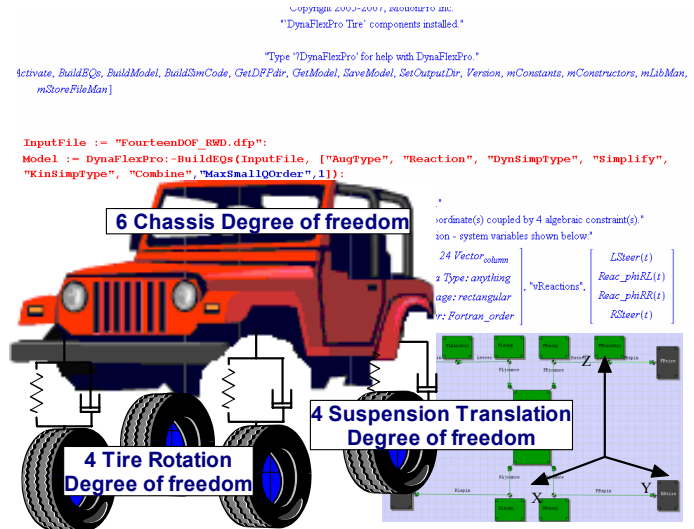


Figure 7: 14 DOF Full Car Ride Vehicle Model D

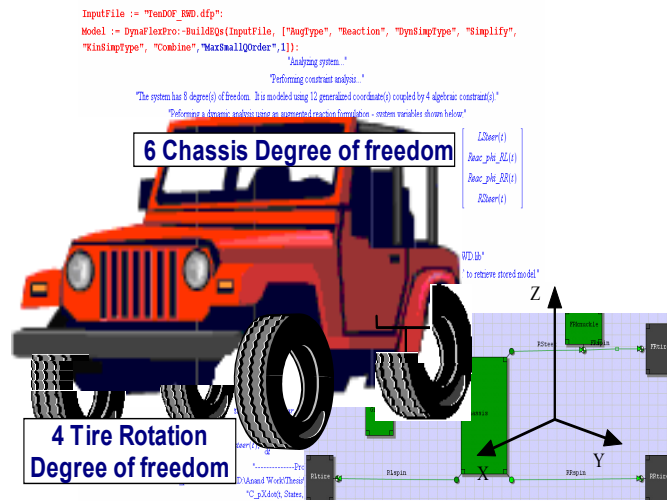


Figure 6: 10 DOF Four Wheel Vehicle w/o Suspension (Model C)

Both models use the Pacejka tire model based upon fitting experimental data to the well-known “magic tire formula”. The code may be easily computed and run as a real time executable with access to various components of tire forces, load transfer in real time while the vehicle maneuvers. Both model C and D were formulated to account for the Ackermann steering angle geometry and compute the reaction forces in the steering joints during simulation, details of which can be seen in [19].

**Steering Force Design:**

In this sub section we will discuss the formulation of the steering force or the rack force which would be reflected through the device to the user as the steering feel.

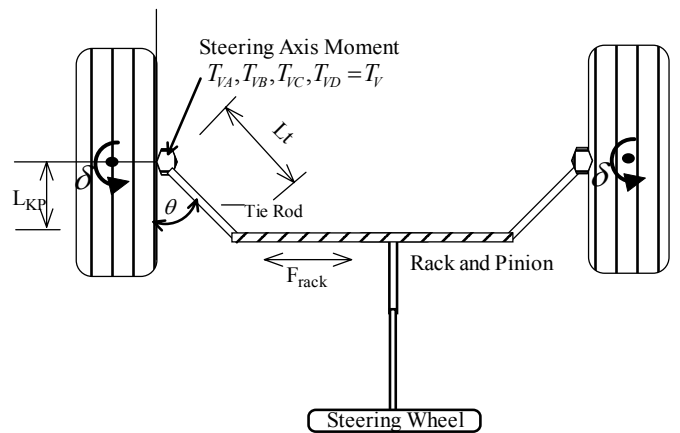


Figure 8: Steering (Rack) Force Estimation

Figure 7 graphically shows the structure of a generic steering system from the top view. The angle  $\delta$  is the angle made by the tires at the road-tire interaction and the angle  $\theta$  is a manufacturer defined tie road offset angle. The rack force or the steering force in the rack and pinion assembly can be computed with Equation (5), [11, 19]

$$F_{rack\_R} = \frac{T_{V\_R}}{L_{KP\_R}}, F_{rack\_L} = \frac{T_{V\_L}}{L_{KP\_L}}, \quad (5)$$

$$F_{rack} = F_{rack\_R} + F_{rack\_L}$$

**Model Validation:**

Model validation is possibly the most important, yet often the most overlooked step in the model building sequence. It was important to select realistic vehicle and tire parameters in order to validate all of the above four models consistently. To this end, we selected vehicle and tire parameters of a large SUV type vehicle to serve as our benchmark (as shown in Table 1).

Parameters	Value	Parameters	Value
Vehicle Mass	2077 Kg	Tire Mass	28 Kg
Vehicle Yaw Inertia	1925 $\text{Kg}\cdot\text{m}^2$	Tire Yaw Inertia	1.56 $\text{Kg}\cdot\text{m}^2$
Track Width	1.555 m	Tire Cornering Stiffness	$-3 \times 10^5$ N/rad
Wheel Base	2.831 m	Tire Radius	0.355 m

**Table 1: Vehicle and Tire Parameters**

Our main tests (Section 5) focus on evaluating driver performance as the vehicle comes off an exit ramp at 10 m/sec (approx. 22 miles/hr). Hence, for consistency, we provide this constant longitudinal speed to all 4 vehicle models in this validation phase while monitoring the response to a square wave steering angle input.

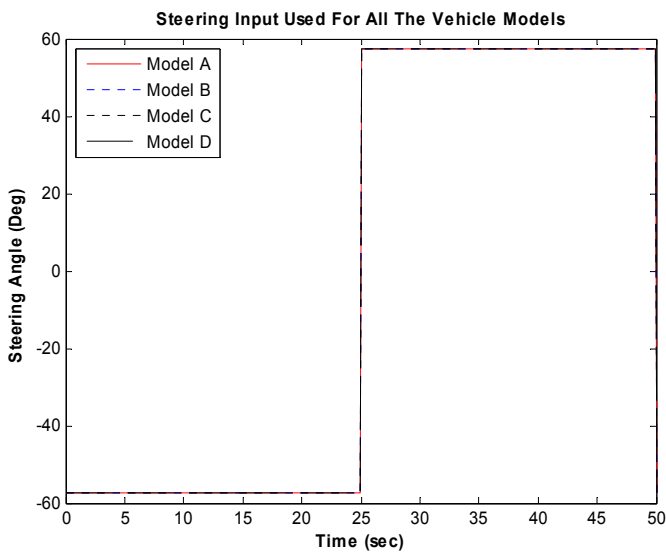


**Figure 9: Steering Input as a Square Wave**

Figure 9 depicts the square wave steering input (57° amplitude and a frequency of 0.04 Hz) was given to a steering system with a steering ratio of 20:1. Figure 10 shows the calculated steering torques (“road feel”) for each of the 4 models that are fed back to the user via the haptic device. We see the torque levels are comparable for all 4 models, with more high frequency effects captured by higher fidelity models. Figure 11 depicts plots of the resultant longitudinal vehicle velocities (which confirm the 10m/s provided). However, we see that the higher order models (such as the Model C-10DOF & Model D-14DOF) capture fluctuations of the vehicle longitudinal velocity when the steering angle changes. Figure 12 now depicts the final trajectories generated by all 4 models which show considerable deviations (despite resulting from the same steering input applied to the same nominal vehicle).

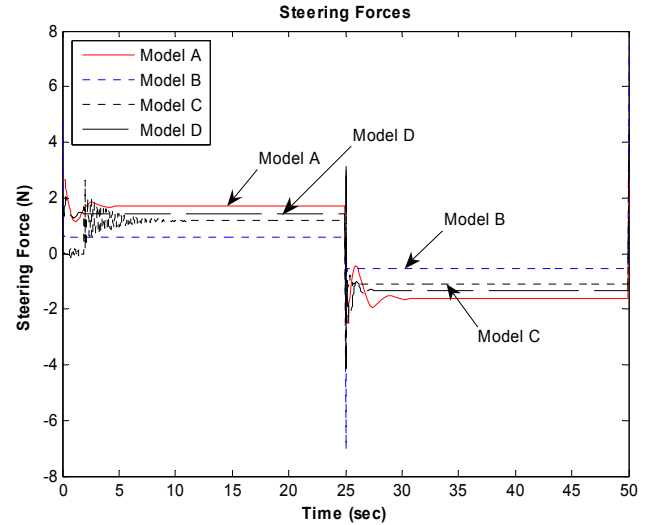


**Figure 10: Steering Force**

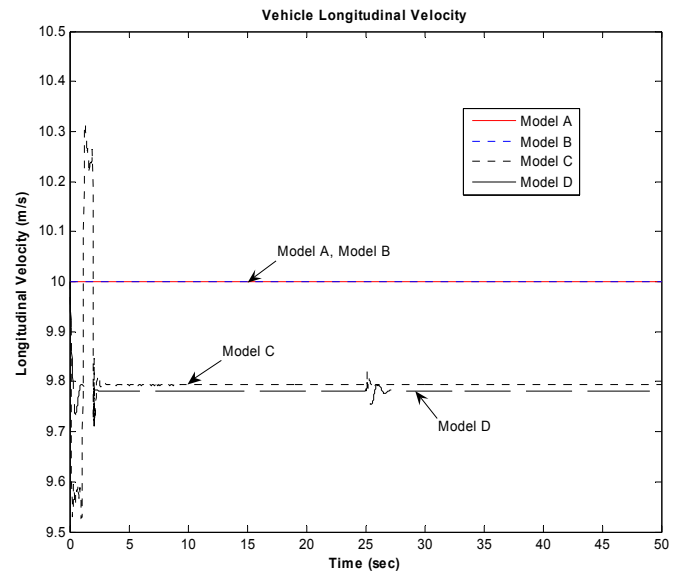


**Figure 11: Longitudinal Velocity of the Vehicle**

### 3. COLLABORATIVE HAPTIC DRIVING

Haptic environments have found many applications for providing tactile and kinesthetic feedback to individual users in diverse arenas from virtual combat simulations to virtual gaming to virtual surgeries. Pedagogical methodologies such as [21], emphasize that students learn best when they are actively engaged in acquiring and constructing knowledge in a learning-by-doing situation.

In recent years the goals have evolved to include multiple individuals with in collaborations/shared haptic virtual environment (VE) which unlocks further potential for training applications. The development and application of methodologies for sharing of an interactive haptic experience with a common virtual object is a focus of active research. We adopt one such method, the virtual teacher [22], developed for

such shared control and study its 3 variants in a collaborative driving tasks.

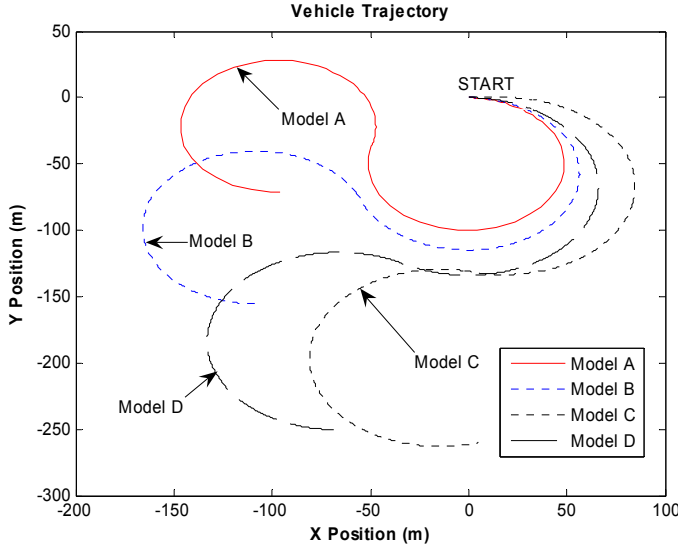


Figure 12: Vehicle trajectories.

In particular, we implement the strategy where an actual human teacher guides a student to learn the task of driving an automobile. The student and teacher perform the task of driving the same vehicle, via 2 separate haptic interfaces. The teacher occasionally resorts to correcting the pupil with a view to improving his/her driving skills in one of the three ways [22]:

Mode I - Indirect Contact: Teacher and pupil each grasp the device (steering wheel) at separate points and thus there is no direct contact between teacher and pupil.

Mode II - Double Contact: Teacher grasps pupil's hand which in turn grasps the device (steering wheel) and thus the pupil experiences a combined effect of vehicle dynamics (steering torque) and the tutor's guidance force.

Mode III - Single Contact: Pupil holds the teacher's hand while the teacher manipulates the system wherein the student will only feel the guidance force from the teacher's actions.

These 3 modes of interaction are illustrated in Figure 13 (a) - (c). Note that while figuratively the vehicle dynamics has been lumped into a single spring damper system, we can provide the user a choice between any of the 4 models (A, B, C or D). We can now compute the vehicle steering torques ( $T_{VA}, T_{VB}, T_{VC}, T_{VD}$ ) as explained in Section 2 and represent them into the forces through the spring damper ( $k_3, b_3$ ). Hence the governing equation (6),

$$\ddot{\delta} I_D = k_2(\theta_2 - \delta) - k_3\delta + b_2(\dot{\theta}_2 - \dot{\delta}) - b_3\dot{\delta} \quad (6)$$

may now be rewritten as:

$$\ddot{\delta} I_D = k_2(\theta_2 - \delta) + b_2(\dot{\theta}_2 - \dot{\delta}) - T_{V(A,B,C)} \quad (7)$$

The reaction torques felt by the teacher  $\tau_1$  in case of the indirect contact mode (Mode I) (Figure 13(a)) is:

$$\tau_1 = -k_1(\theta_1 - \theta_2) - b_1(\dot{\theta}_1 - \dot{\theta}_2) \quad (8)$$

As we can see the student acts as a motion and force sensor between the teacher and the vehicle. Similarly, the reaction torques felt by the student  $\tau_2$ :

$$\tau_2 = k_1(\theta_1 - \theta_2) - k_2 \cdot (\theta_2 - \theta_3) + b_1(\dot{\theta}_1 - \dot{\theta}_2) - b_2(\dot{\theta}_2 - \dot{\theta}_3) \quad (9)$$

The system equations for all of the above three cases are discussed in greater detail in [19].

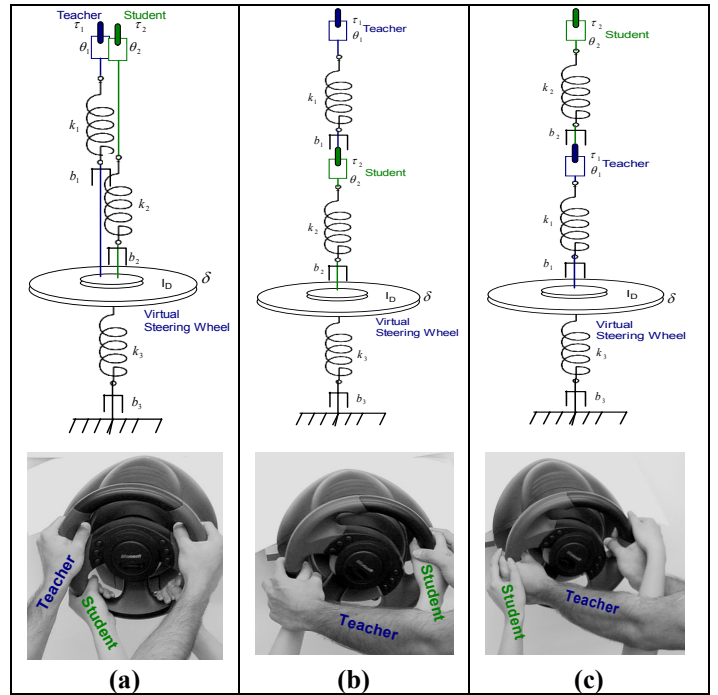


Figure 13: (a) Indirect Contact Mode ( Mode I ). (b) Double Contact Mode ( Mode II ), and (c) Single Contact Mode ( Mode III ).

#### 4. IMPLEMENTATION

We examine the development of an analysis framework for virtual simulation of an automotive vehicle and validation of the various haptic collaboration modes. The mathematical formulation of the various vehicle dynamics models are implemented within a real-time HIL simulation using MATLAB/SIMULINK/RTW. A Graphical User Interface (GUI) was created to permit the selection between the four vehicle dynamics models, three interaction modes for haptic collaboration and the multiple sets of haptic devices.

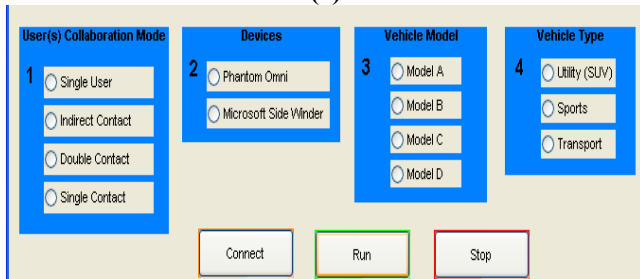
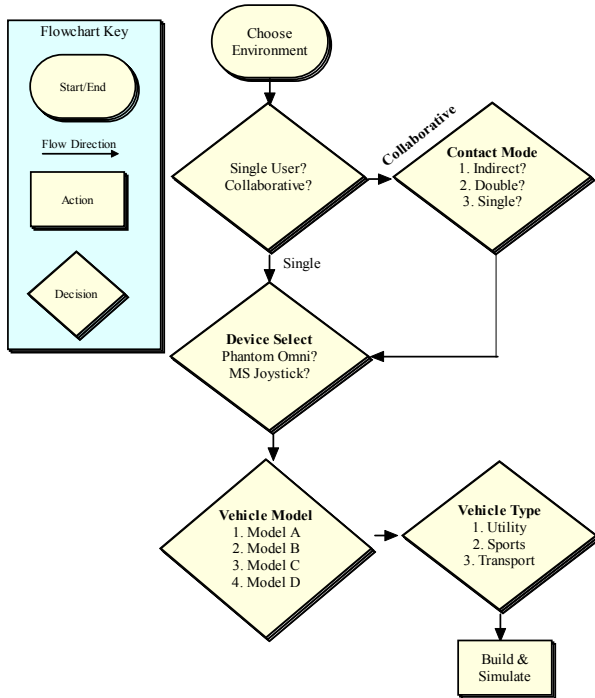


Figure 14: (a) Simulation Flowchart (b) Developed GUI for parameter selection (Ver.1)

Figure 14(a) shows the logical sequence of user actions facilitated by the GUI shown in Figure 14(b). Currently we can deploy either of 2 HIL devices, the Sensable’s Phantom Omni and the Microsoft Joystick which are interfaced through a IEEE-1394 compliant FireWire® port. Software interface for real-time control, at high sample rates, is achieved using the ProSense SDK from HandShake VR, Inc. The drag and drop construction in block diagrammatic form, shown in Figure 15 together with the encapsulation and code generation simplifies our deployment allowing us to focus on higher level issues. In particular, we can now pursue comparative parametric analyses such as studying the role of “vehicle types” (with varied inertias as shown in Table 2) or study the effects of single user vs. collaborative control (as shown in Figure 13).

Vehicle Type	Tunable Parameters	
	Yaw Inertia	Steering Ratio
SUV Utility	1925 $kg \cdot m^2$	20:1

Sports	1660 $kg \cdot m^2$	15:1
Transport	6320 $kg \cdot m^2$	50:1

Table 2: Vehicle Type Selection

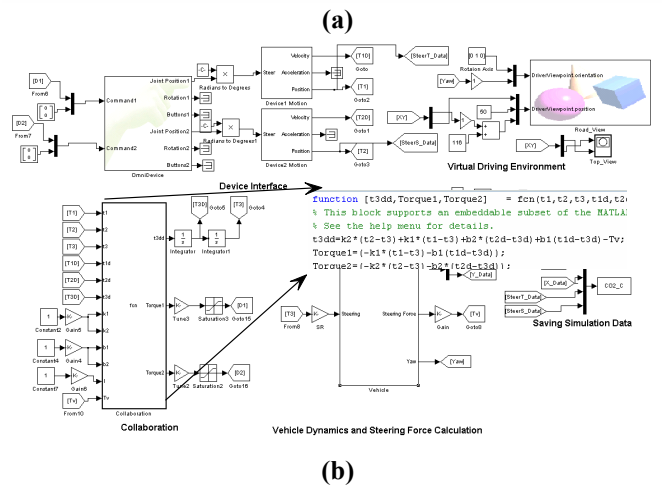
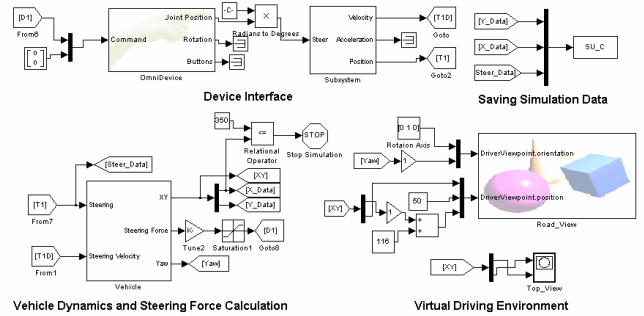
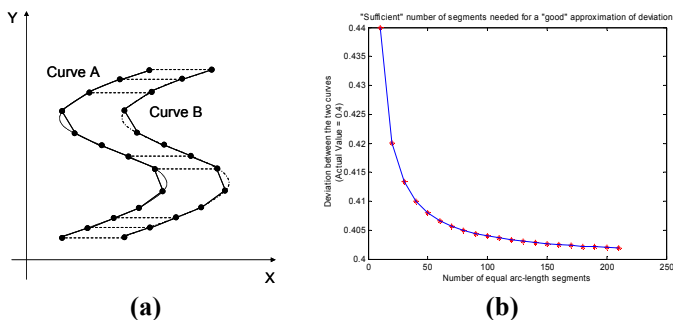


Figure 15: Simulink Models (a) Single User and (b) Collaborative User Environment.

## 5. EXPERIMENTAL SETUP AND RESULTS

Our implementation allows us to test various scenarios based on the selection of: (i) User Collaboration Modes (Single user, Collaborative Modes I - III), (ii) Input devices (Phantom Omni or Microsoft Force-Feedback Joystick), (iii) Vehicle Models (A, B, C or D), and (iv) Vehicle Types (Utility, Sports, and Transport). In this paper, however, we will focus on the evaluation of the combination of (i) User collaboration modes with (iii) Vehicle models, while restricting the device to ‘Phantom Omni’ and vehicle type to ‘Utility’.

To quantify the driving performance of the subject, we adopted the Error Value Parameter (EVP) measure. The Error Value Parameter (EVP), shown in Figure 16 was developed in [23] to closely resemble and complement the Structural Error Metric used in mechanism synthesis [24]. The EVP is a normalized quantity that measures the discrepancy between the desired path and the subject generated path at equal arc-length correspondence points. A low EVP indicates low path following error and hence a better driving performance. The trajectory history from the EVP serves as our preliminary assessment measure to evaluate the driver performance with various vehicle models.



**Figure 16: (a) Error Value Parameter computed as the normalized Euclidean distance between equal-arc-length correspondence points; (b) EVP between two curves v/s the number of equal-arc-length segments**

For the initial testing phase, a sinusoidal path of amplitude 10 m and frequency of 0.003 Hz was chosen. Subjects were required to guide the “vehicle” along this path, trying to travel as close as possible to the center line, with a constant longitudinal velocity of 10 m/sec. For the preliminary testing, the test group consisted of 5 subjects in the 25-30 year age group. The subjects considered were of normal health, had similar driving backgrounds and did not vary significantly in height and weight. This testing is intended to be the precursor to a more thorough and comprehensive study.

To minimize variations due to the drivers seating position the following guidelines were followed. Shoulder and elbow flexion angle were maintained close to 90° while the height of the chair and the distance from the Phantom Omni device was adjusted to maintain a fixed offset. The subjects were asked to grip the Phantom Omni device as shown in the experiment setup photo in Figure 17(a)-(b).

In our preliminary study, all tests were conducted using Phantom Omni devices with a sampling time of 3 milliseconds. All subjects were asked to drive along the same path for the sixteen experiments as shown in Table 3. The tests were conducted on each subject at a stretch without any rest breaks, since all the tests were of a short duration.

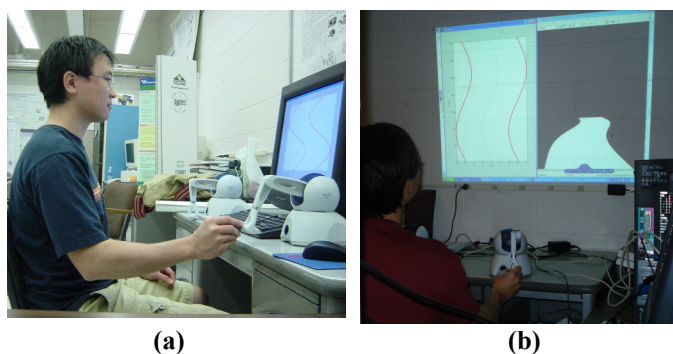


**Figure 17: (a) Experiment setup side view and (b) Subject driving in a single user environment.**

	Model A	Model B	Model C	Model D
Single User	Exp. 1	Exp. 2	Exp.3	Exp. 4

Collaboration Mode I	Exp. 5	Exp. 6	Exp. 7	Exp. 8
Collaboration Mode II	Exp. 9	Exp. 10	Exp. 11	Exp. 12
Collaboration Mode III	Exp. 13	Exp. 14	Exp. 15	Exp. 16

**Table 3: Design of Experiments**

In the post processing, the user trajectories were parameterized using the arc length parameterization and the Error Value Parameter (EVP) was calculated [25]. Figure 18 (a) shows representative trajectories for subject 3, using Model A, B and C and D in a single user environment. Figure 18 (b) is the calculated EVP measure for a given subject for each of the four models.

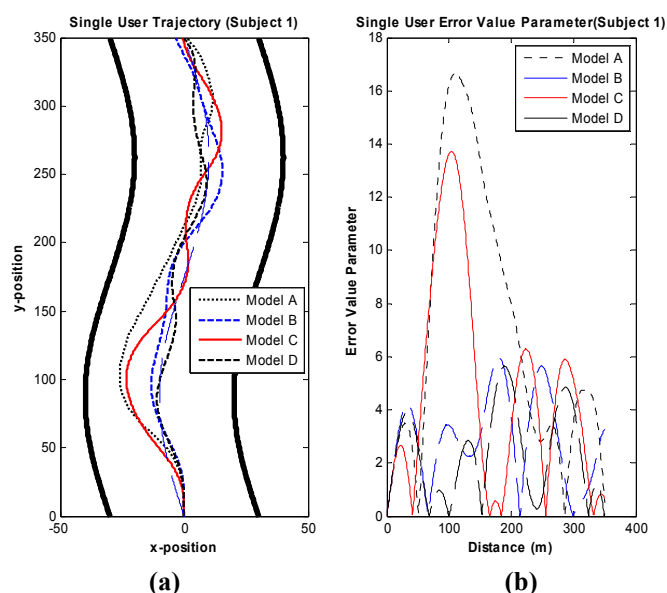


**Figure 18: (a) User trajectory with various vehicle models and (b) EVP measure with various vehicle models.**

Figure 18 shows a visual representation of a subject’s path following error for a particular location on the path that can be further processed with other statistical measures. For example, a cumulative EVP measure can be generated as the sum of the EVP over an entire path. We use this measure to provide us with a means to compare user performance for various collaboration modes and with the varying vehicle dynamics models. Figure 19 depicts the cumulative EVP for Subject 1 for all 16 experiments that allows for such a comparative performance evaluation.

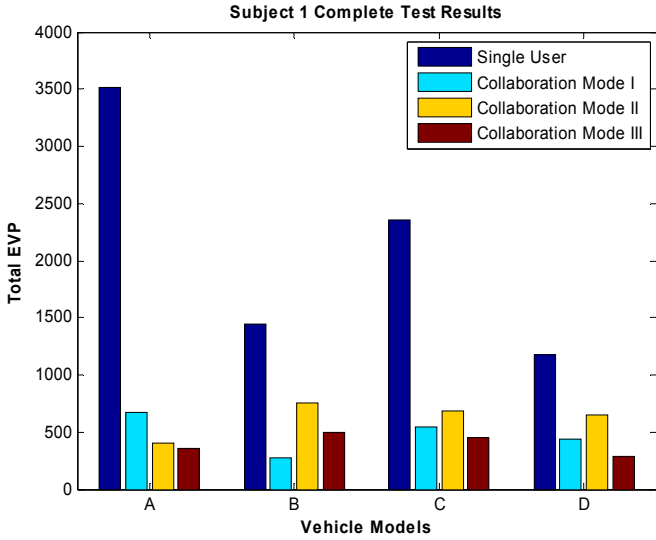
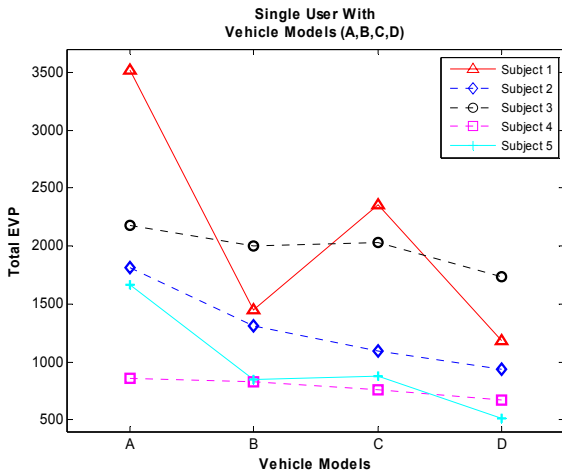


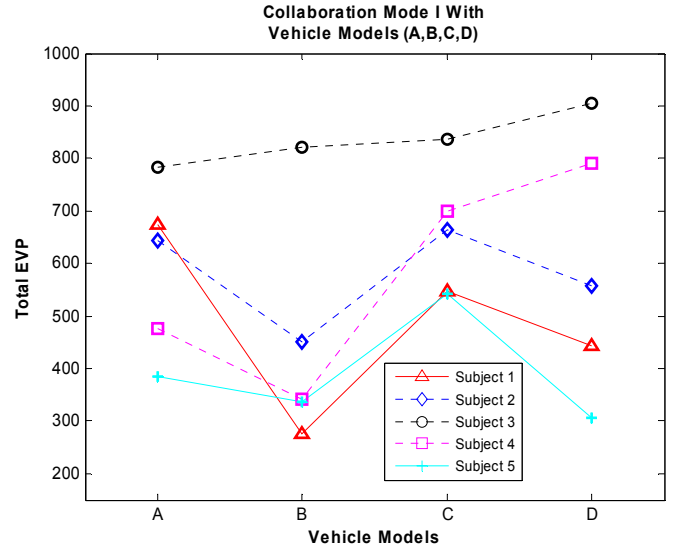
Figure 19: Total EVP for vehicle model A, B, C and D with all 4 modes of driver interactions.

For example, some improvements in driver performance can be seen as higher fidelity models are used as borne out in all 4 modes of driver interactions (Single, Collaborative Mode I, II, III).

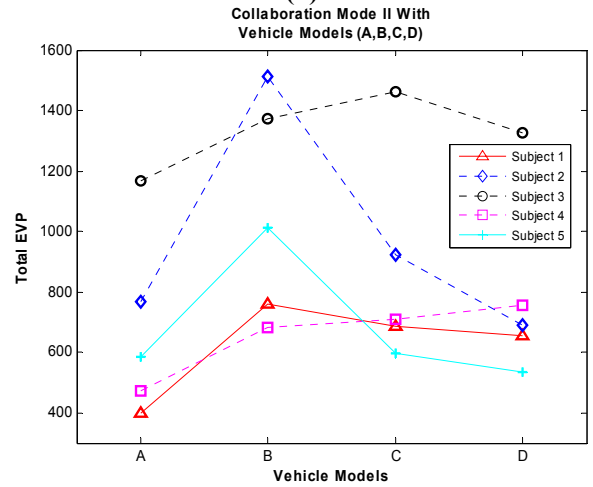
In order to understand this behavior, we will visualize the above information with several comparative line charts to compare user performance across all four vehicle models.



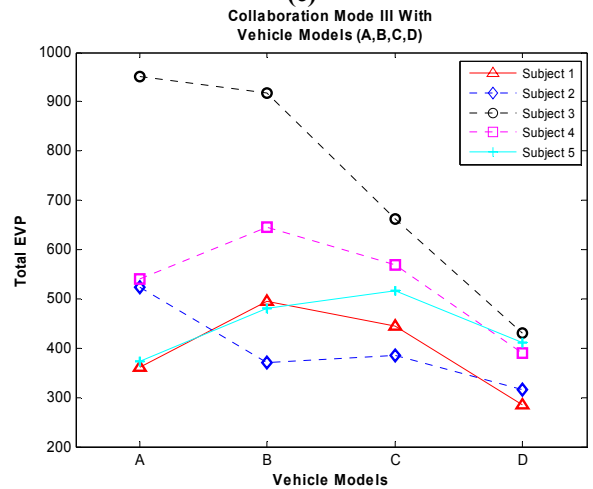
(a)



(b)



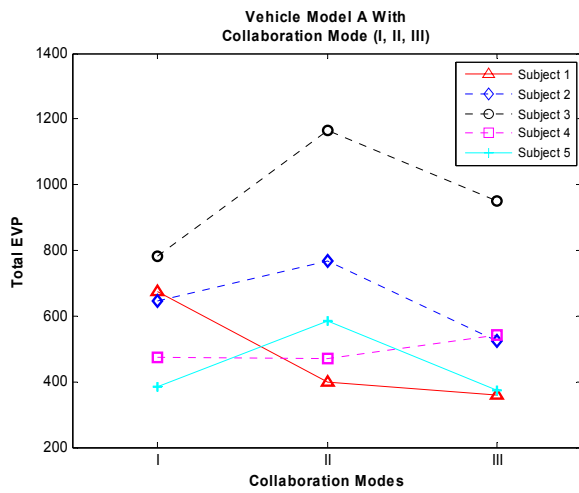
(c)



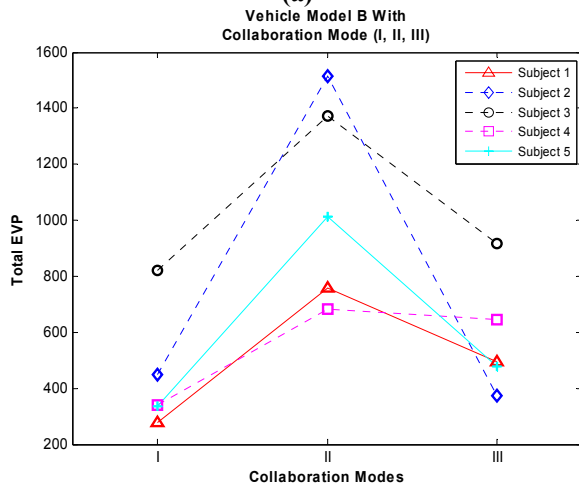
(d)

Figure 20: : EVP Measure for (a) Single User Environment, (b) Collaborative Mode I, (c) Collaborative Mode II, (d) Collaborative Mode III, with all Four Vehicle Models.

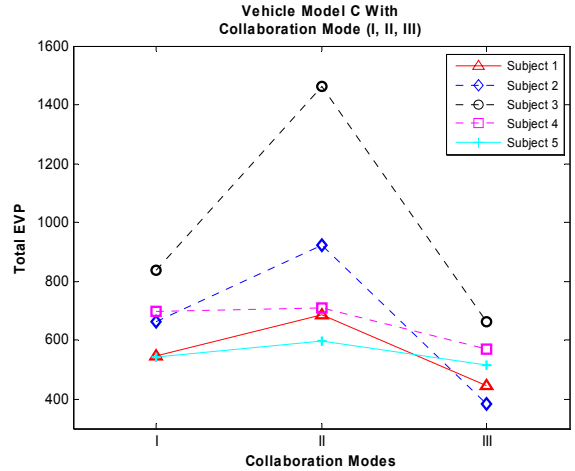
As can be seen from Figure 20 (a), all users unanimously performed their best with the Model D in the single user environment. In case of Figure 20 (b), with the exception of Subject 5 all others performed better with vehicle Model B. Subject 5 performed the best with Model D. However, this performance difference between Model B and D with Subject 5 is very small and hence it could be said that with Collaboration Mode-I users prefer driving with vehicle model B. Following that as seen from Figure 20 (c) with the exception of Subject 2 and 5 all others performed better with vehicle Model A in Collaboration Mode-II. Subject 2 and 5 performances were once again proven to be the best with Model D in Collaboration Mode-II. Finally, from Figure 20 (d), once again with the exception of Subject 5 all other showed their best performance while driving vehicle model D in Collaborative Mode III.



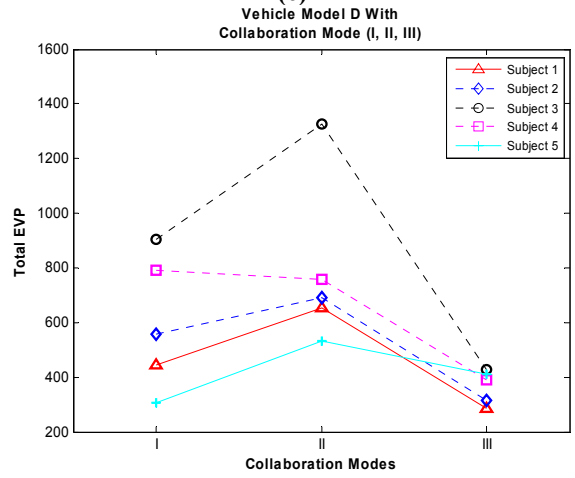
(a)



(b)



(c)



(d)

Figure 21: Comparison of all single user and collaborative environment for average of all vehicle models.

To examine and visualize the effects of specific collaborative models with individual vehicle models we plotted our results in the manner as shown in Figure 21 (a)–(d). As can be seen from Figure 21 (a), with the exception of Subject 4 and 3 all users preferred Collaborative Mode-III while using Model A. Figure 21 (b) depicts that Collaborative Mode-I unanimously brought out the best performance amongst all the users while driving with Model B. Similarly, all users without any exceptions once again preferred driving Model C using Collaborative Mode-III as can be seen from Figure 21 (c). Finally, Figure 21 (d) shows that Collaboration Mode-III is again the preferred mode when driving with Model D with the exception of Subject 5 who preferred Collaboration Mode-I in this case.

## 6. DISCUSSION AND CONCLUSION

The SBW paradigm shows enormous promise to simplify the implementation of shared collaborative control of driving tasks. Hence we developed a HIL Haptically-Enabled

simulation framework to facilitate the validation and testing of various aspects of the SBW paradigm.

While not statistically significant, the comparison charts provided below are intended to provide a better visualization of the outcomes of the prior testing. Table 4 provides number of users who had minimum EVP value for a particular vehicle model and collaboration mode and therefore better performance while driving.

Vehicle Models	A	B	C	D
Single User	0	0	0	5
Collaboration Mode – I	0	4	0	1
Collaboration Mode – II	3	0	0	2
Collaboration Mode – III	1	0	0	4

**Table 4: Vehicle Model User Performance Chart**

As can be seen (Table 4) all users showed minimum EVP i.e. better performance with Model D in the single user environment. Four user performed better while driving vehicle model B in Collaborative Mode-I. However, users showed mixed performance while driving in Collaborative Mode-II. In particular, three user performed better with model A and two performed better with model D. Finally, four users performed better with vehicle model D while driving in Collaborative Mode-III. In general from the EVP comparison it can be said that users performed better with Model D in most of the cases as compared to other vehicle models.

Furthermore, the fact that different users prefer different collaboration mode is born out while comparing multi-user collaboration modes (Figure 21 a-d). Table 5 shows this preferential selection of collaboration modes per user in tabulated form.

Collaboration Mode	I	II	III
Vehicle Model A	2	0	3
Vehicle Model B	5	0	0
Vehicle Model C	0	0	5
Vehicle Model D	1	0	4

**Table 5: Collaboration Mode User Performance Chart**

Subjects performed better with Collaboration Mode I and III while driving with Model A. All subjects in case of Model B and C preferred Collaboration Mode I and III respectively. Four subjects preferred Collaboration Mode III in case of vehicle Model D. One consistent observation that can be inferred from Table 5 is that no users preferred Collaboration Mode II while driving any of the four vehicle models which is where the teacher holds the students hand that in turn steers the wheel.

To conclude, we implemented and presented preliminary results from evaluation of various modes of collaborative

control of driving with varying fidelity of vehicle dynamics simulations. The Error Value Parameter metric/measure was analyzed to quantitatively determine user performance while driving varying fidelity vehicle models in single user, multi-user collaboration modes. These comparisons presented are intended to be precursors to a full fledged human factor parametric experimental study. Further studies with detailed parametric evaluations would be necessary to better understand and validate such hypothesis.

## 7. ACKNOWLEDGMENTS

We gratefully acknowledge the support from National Science Foundation CAREER Award (IIS-0347653) for this research effort.

## 8. REFERENCES

1. Yih, P. and J.C. Gerdes. *SBW for vehicle State Estimation and Control*. in *Advanced Vehicle Estimation Control*. 2004.
2. Bretz, E., *By-Wire Cars Turn The Corner* in *IEEE Spectrum magazine*. 2001. p. 60-73.
3. Isermann, R., R. Schwarz, and S. Stolzl, *Fault-Tolerant Drive-by-Wire Systems*, in *IEEE Control Systems Magazine*. 2002.
4. Bertoluzzo, M., et al., *An Approach To Steer-by-Wire System Design*. IEEE, 2005.
5. Amberkar, S., et al., *A Control System Methodology For Steer By Wire Systems*. SAE International, 2004.
6. Srinivasan, M., *What Is Haptics*. 1995, Massachusetts Institute of Technology.
7. Nishino, H., et al. *A Distributed Virtual Reality Framework for Korea-Japan High-Speed Network Testbed*. in *IEEE Proceedings of the 20th International Conference on Advanced Information Networking and Applications*. 2006.
8. Lawrence, D., *Stability And Transparency In Bilateral Teleoperation*. IEEE Transactions on Robotics and Automation, October 1993. **9**(5): p. 624-637.
9. Ansari, A., *Vehicle Steering System Having Master/Slave Conguration and Method* in *US Patent*. 2001: US.
10. Kelber, C., et al. *Active Steering Unit With Integrated ACC For X-by-Wire Vehicles Using a Joystick as H.M.I*. in *IEEE Intelligent Vehicles Symposium*. 2004. Parma, Italy.
11. Ryu, J. and H. Kim, *Virtual Environment for Developing Electronic Power Steering and Steer-by-Wire Systems*. IEEE, Robots and Systems, 1999.
12. Liu, A. and S. Chang, *Force Feedback In A Stationary Driving Simulator*, Nissan Cambridge Basic Research: Cambridge, MA.
13. Odenthal, D., et al. *How To Make Steer-by-Wire Feel Like Steering*. in *15th Triennial World Congress*. 2002. Barcelona, Spain (2002).
14. Yih, P., *Steer-By-Wire: Implications For Vehicle Handling And Safety*, in *Department of Mechanical Engineering*. 2005, Stanford University.

15. Genta, G., *Motor Vehicle Dynamics*. 1997: World Scientific.
16. Gillespie, T., *Fundamentals of Vehicle Dynamics*. 1992: SAE, Inc.
17. Rajamani, R., *Vehicle Dynamics and Controls*. 2005: Springer.
18. Milliken, W. and D. Milliken, *Race Car Vehicle Dynamics*. 1995: SAE International, Inc
19. Naik, A., *Role of Vehicle Dynamic Modeling Fidelity with Haptic Collaboration in SBW systems*, in *Mechanical and Aerospace Engineering*. 2007, The State University of New York at Buffalo Buffalo.
20. *MotionPro Inc DynaFlexPro-Tire*, MapleSoft Waterloo, CA.
21. Miao, Y., N. Pinkwart, and H. Hoppe, *A Collaborative Virtual Environment For Situated Learning Of Car Driving*, University of the Netherlands, Carnegie Mellon University, University of Duisburg-Essen.
22. Gillespie, R. and S. O'Modhrain, *The Virtual Teacher*. ASME International Mechanical Engineering Congress: Dynamic Systems and Control Division, 1998 Vol 2, (Haptic Interfaces for virtual Environments and Teleoperator Systems) DSC-Vol.60.
23. Krovi, V., *Design and Virtual Prototyping of User-Customized Assistive Devices*, in *Department of Mechanical Engineering and Applied Mechanics*. 1998, University of Pennsylvania.
24. Sandor, G. and A. Erdman, *Advanced Mechanism Design: Analysis and Synthesis*. Vol. 2. 1984, Englewood Cliffs, NJ: Prentice-Hall.
25. Nair, P., *Development of Quantitative Measures for Characterization of Upper Limb Dysfunction*, in *Mechanical & Aerospace Engineering*. Feb. 2004., SUNY at Buffalo.